The Generalized Parton Distributions program in Hall A at Jefferson Lab

C. Munoz Camacho

The Generalized Parton Distribution program in Hall A at Jefferson Lab

C. Muñoz Camacho

LPC Clermont-Ferrand CNRS/IN2P3, F-63177 Aubière, France

Abstract. Recent results on the Generalized Parton Distribution (GPD) program at Jefferson Lab (JLab) will be presented. The emphasis will be in the Hall A program aiming at measuring Q^2-dependences of different terms of the Deeply Virtual Compton Scattering (DVCS) cross section. This is a fundamental step before one can extract GPD information from JLab DVCS data. Neutral pion production will also be discussed and results from the CLAS collaboration will be shown. Finally, the upcoming program in Hall A, using both a 6 GeV beam ($\approx$ 2010) and a 11 GeV beam ($\approx$ 2015) will be described.

Keywords: Generalized Parton Distributions (GPDs), Exclusive reactions.
PACS: 13.60.Fz, 13.40.Gp, 14.20.Dh, 13.60.Hb

INTRODUCTION

Measurements of electro-weak form factors determine nucleon spatial structure, and deep inelastic scattering (DIS) of leptons off the nucleon measures parton distribution functions, which determine longitudinal momentum distributions. The demonstration by Ji [1], Radyushkin [2], and Müller *et al.* [3], of a formalism to relate the spatial and momentum distributions of the partons allows the exciting possibility of determining spatial distributions of quarks and gluons in the nucleon as a function of the parton wavelength. These new structure functions, now called generalized parton distributions (GPD), became of experimental interest when it was shown [1] that they are accessible through deep virtual Compton scattering (DVCS) and its interference with the Bethe-Heitler (BH) process (Fig. 1). The factorization proofs [4, 5] confirmed the connection between DVCS and DIS. Diehl *et al.* [6] showed that the twist-2 and twist-3 contributions in the DVCS-BH interference terms (the first two leading orders in a $1/\sqrt{Q^2}$ expansion) could be extracted independently from the azimuthal-dependence of the helicity-dependent cross section. Burkardt [7] showed that the *t*-dependence of the GPDs is the Fourier conjugate to the transverse spatial distribution of quarks in the infinite momentum frame as a function of momentum fraction. Ralston and Pire [8], Diehl [9] and Belitsky *et al.* [10] extended this interpretation to the general case of skewness $\xi \neq 0$.

CURRENT EXPERIMENTAL SITUATION

These concepts stimulated an intense experimental effort in DVCS. The H1 [11, 12] and ZEUS [13] collaborations measured the cross section for $x_B \approx 10^{-3}$. The HERMES collaboration measured relative beam-helicity [14] and beam-charge asymmetries [15, 16].

Relative beam-helicity [17] and longitudinal target [18] asymmetries were measured at the Thomas Jefferson National Accelerator Facility (JLab) by the CLAS collaboration. The first dedicated DVCS experiment ran in Hall A at JLab [19]. Helicity-correlated cross section of electroproduction of photons were measured with high statistical accuracy as a function of Q^2 (Fig. 2).

The combination of Compton form factors (CFF) extracted from these data (Fig. 3) was found to be independent of Q^2, within uncertainties. This exciting result strongly supports the twist-2 dominance of the imaginary part of the DVCS amplitude. GPDs can then be accessed experimentally at the kinematics of JLab.

A dedicated DVCS experiment on the neutron (E03-106) followed E00-110. Using a deuterium target, E03-106 provided the first measurements of DVCS on the neutron, particularly sensitive to the least known GPD E, and DVCS on the deuteron [20]. A first constraint on the orbital angular momentum of quarks inside the nucleon (Fig. 4) was obtained relying on the VGG model of GPDs [21].

Deep neutral meson production

The π^0 electroproduction longitudinal cross section provides an extremely interesting access to GPDs. Indeed, if factorization applies, it provides a promising way to perform a flavor separation of GPDs. Moreover, π^0 production probes only the "polarized" GPDs in the nucleon ($\tilde{H}$ and $\tilde{E}$), which contain information about the spatial distribution of the quark spin. This complements DVCS measurements, where all GPDs participate. E00-110 measured the π^0 electroproduction cross section at $Q^2 = 2.3$ GeV^2 and $E_b = 5.75$ GeV. From the azimuthal dependence of the cross section, 3 interference cross sections (σ_{LT}, σ_{TT} and $\sigma_{LT'}$) and the combination $\sigma_T + \varepsilon\sigma_L$ were extracted. E00-110 could not perform an L/T separation of the cross section in order to access the longitudinal part that is (potentially) related to GPDs. However, in a future approved experiment (E07-007 [22]), the σ_L contribution will be isolated for three different bins in Q^2, and therefore we will measure all 5 independent cross sections as a function of Q^2. This will provide, for the first time, a test of factorization for the longitudinal π^0 cross section and thus demonstrate (or not) the feasibility of extracting GPD data from this interesting channel.

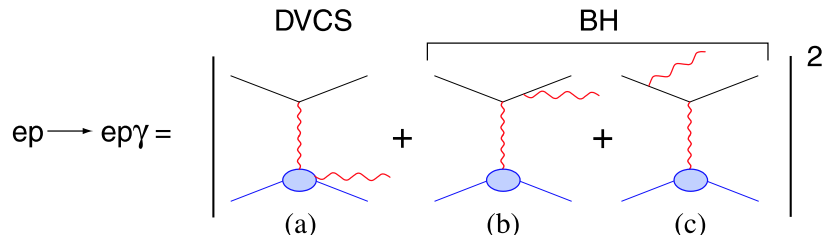The CLAS collaboration has recently published beam spin asymmetries (BSA) for π^0

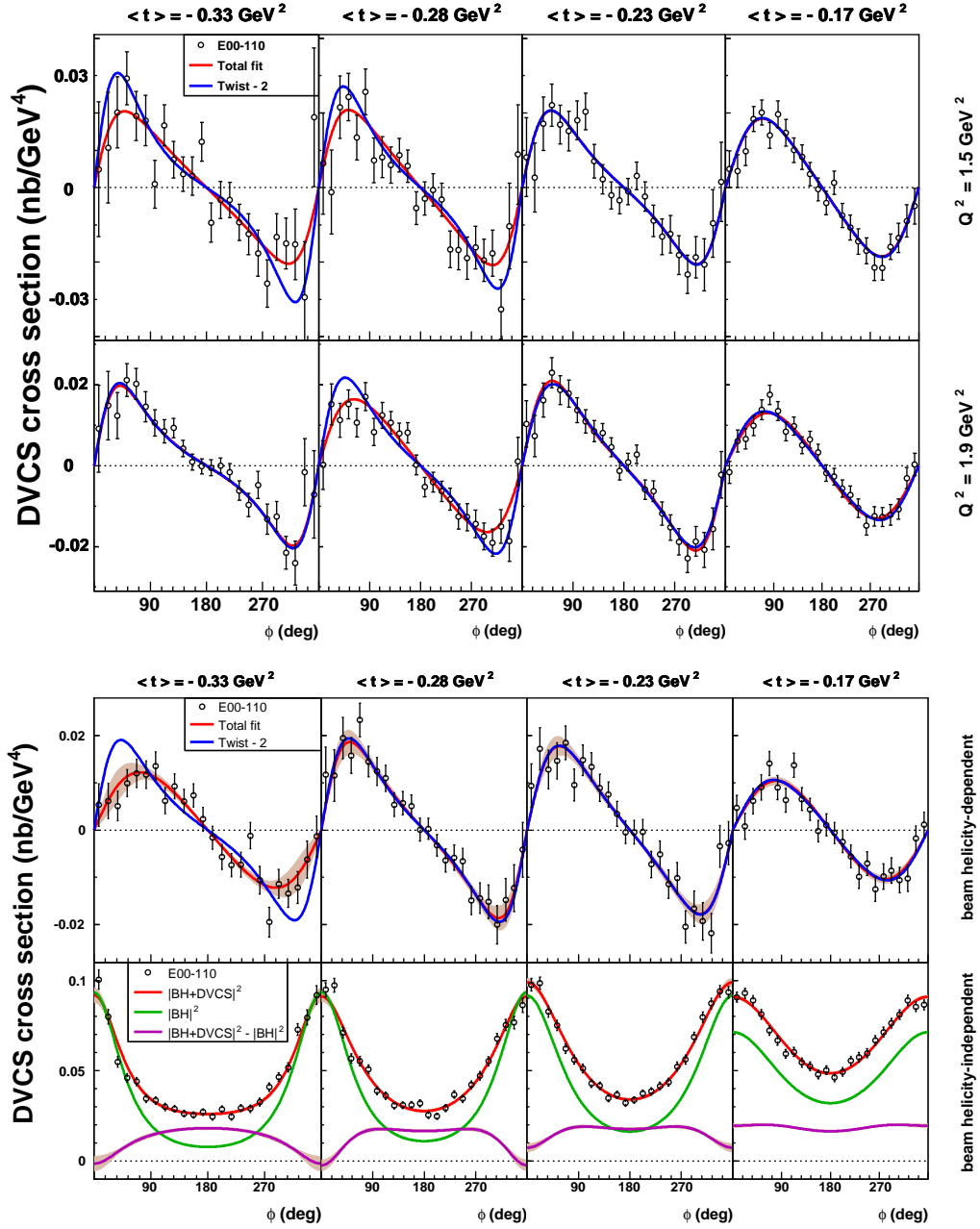**FIGURE 1.** DVCS and BH processes: the two interfering contributions to the electroproduction of photons.

FIGURE 2. Data and fit to the helicity-dependent $d^4\Sigma/dQ^2dx_Bdtd\phi$, and the helicity-independent $d^4\sigma/[dQ^2dx_Bdtd\phi]$ cross sections, as a function of the azimuthal angle ϕ between the leptonic and hadronic planes. All bins are at $\langle x_B \rangle = 0.36$. Error bars show statistical uncertainties. Solid lines show total fits with one-σ statistical error bands. The green line is the $|BH|^2$ contribution to $d^4\sigma$. The first three rows show the helicity-dependent cross section for values of $Q^2 = 1.5, 1.9$ and 2.3 GeV^2, respectively. The last row shows the helicity-independent cross section for $Q^2 = 2.3$ GeV^2.
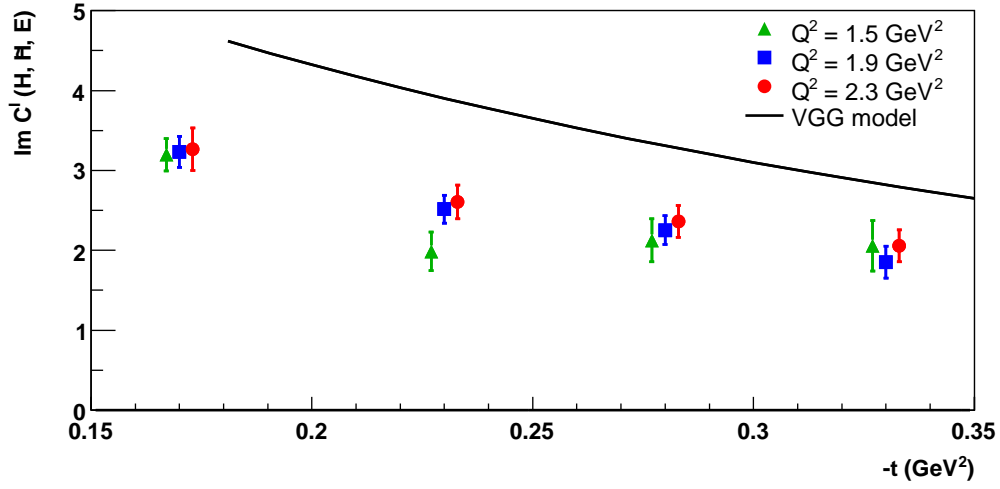
FIGURE 3. Extracted imaginary part of the twist-2 angular harmonic as function of t. Superposed points are offset for visual clarity. Their error bars show statistical uncertainties.
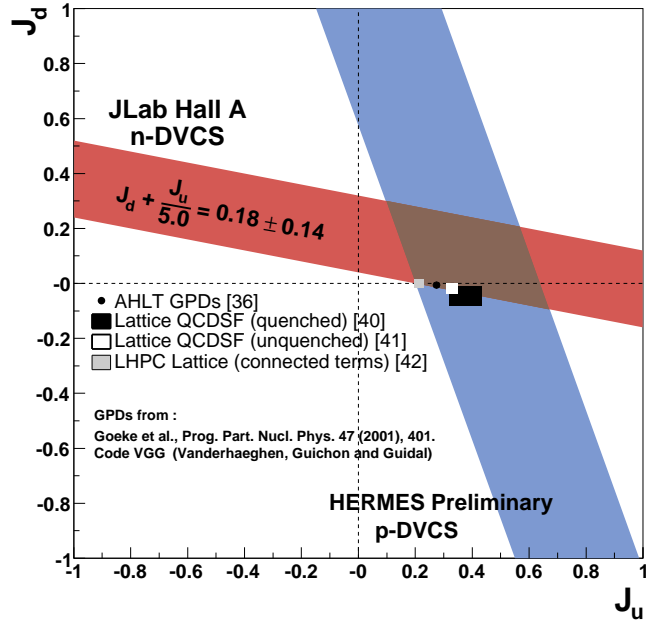

FIGURE 4. Experimental constraint on J_u and J_d quark angular momenta from the present n-DVCS results [20]. A similar constraint from the p-DVCS target spin asymmetry measured by HERMES, and different lattice QCD based calculations are also shown.

electroproduction [23]. Fig. 5 (left) shows the kinematic coverage of the data and the BSA as a function of ϕ for a typical kinematic bin. The BSA can be written as:

$$BSA = \frac{\overrightarrow{\sigma} - \overleftarrow{\sigma}}{\overrightarrow{\sigma} + \overleftarrow{\sigma}} = \frac{\alpha \sin \phi}{1 + \beta \cos \phi + \gamma \cos 2\phi}$$
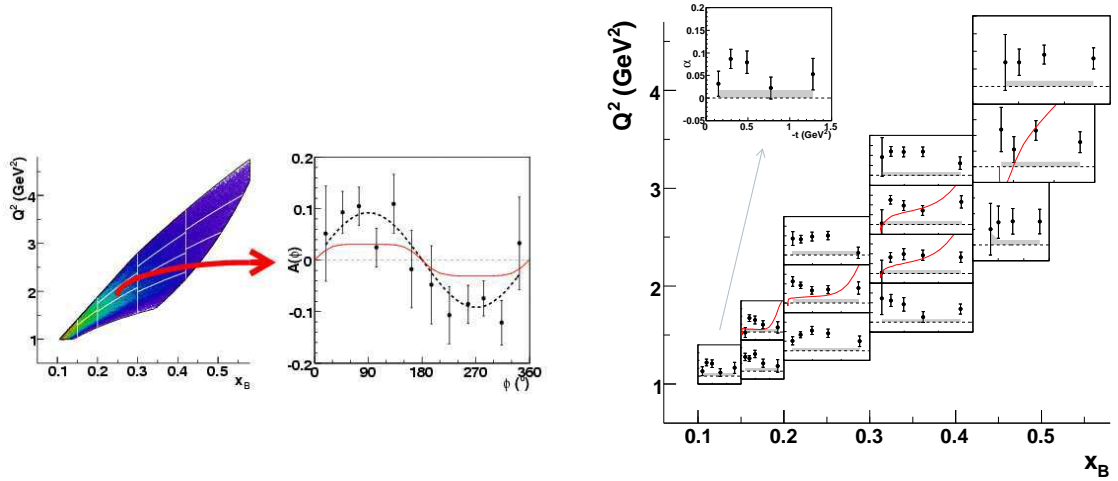
FIGURE 5. Kinematic coverage and typical BSA as a function of ϕ for π^0 electroproduction, as measured by the CLAS collaboration [23] (left). The parameter A from a fit by the function $A\sin\phi$ is shown on the right for each bin in Q^2, x_B and t.

with

$$\alpha = \frac{\sqrt{2\varepsilon(1-\varepsilon)}\sigma_{LT'}}{\sigma_T + \varepsilon\sigma_L}$$

Fig. 5 (right) shows the results of the parameter A of a fit of experimental BSA by the expression $A\sin\phi$, which reproduces well the shape of the data. A non-zero BSA indicates a non-zero value of $\sigma_{LT'}$.

FUTURE DVCS PROGRAM WITH CEBAF AT 6 GEV

A new experiment E07-007 was recently approved with the highest scientific rating (A) by the JLab Program Advisory Committee (PAC-31) and will run in the next 2–3 years. E07-007 will use the important lessons we learned in E00-110 to further test and explore the potential of DVCS to measure GPDs.

In E00-110 we managed to determine the photon electroproduction helicity-independent (unpolarized) cross section. This additional information was not in the initial goal of the E00-110 experiment, and we were only able to measure it at one single value of $Q^2 = 2.3$ GeV^2 (Fig. 2). We found that the total cross section was much larger than the BH contribution. The excess in the cross section is then coming from both the interference term (BH–DVCS) and the DVCS^2 contribution. These contributions contain different kinds of GPD combinations. The interference term is proportional to a *linear* combination of GPD integrals, whereas the DVCS^2 is related to a *bilinear* combination of GPD integrals.

The harmonic ϕ structure of the DVCS cross section does *not* allow the independent determination of the BH-DVCS interference and the DVCS^2 contributions. Indeed, the interference $\mathscr{I}$ and DVCS^2 terms have the following harmonic structure (with

$Q = \sqrt{Q^2}$):

$$\mathscr{I} = \frac{i_0/Q^2 + i_1\cos\varphi/Q + i_2\cos 2\varphi/Q^2 + i_3\cos 3\varphi/Q}{\mathscr{P}_1\mathscr{P}_2}$$

$$\text{DVCS}^2 = d_0/Q^2 + d_1\cos\varphi/Q^3 + d_2\cos 2\varphi/Q^4. \tag{1}$$

The product of the BH propagators reads:

$$\mathscr{P}_1\mathscr{P}_2 = 1 + \frac{p_1}{Q}\cos\varphi + \frac{p_2}{Q^2}\cos 2\varphi. \tag{2}$$

Reducing to a common denominator ($\times \mathscr{P}_1\mathscr{P}_2$), one obtains:

$$\begin{aligned}
\mathscr{P}_1\mathscr{P}_2\mathscr{I} + \mathscr{P}_1\mathscr{P}_2\text{DVCS}^2 = &\ \boxed{(i_0+d_0)/Q^2} + d_1 p_1/2/Q^4 + p_2 d_2/2/Q^6 \\
&+ [i_1/Q + (p_1 d_0 + d_1)/Q^3 + (p_1 d_2 + p_2 d_1)/2/Q^5]\cos\varphi \\
&+ [i_2/Q^2 + (p_2 d_0 + p_1 d_1/2 + d_2)/Q^4]\cos 2\varphi \\
&+ [i_3/Q + (p_1 d_2 + p_2 d_1)/2/Q^5]\cos 3\varphi \\
&+ [p_2 d_2/4/Q^6]\cos 4\varphi.
\end{aligned} \tag{3}$$

One sees in Eq. (3) that the interference $\mathscr{I}$ and the DVCS^2 terms *mix at leading order in 1/Q* in the azimuthal expansion.

Interference and DVCS^2 separation

E07-007 was approved to measure the photon electroproduction helicity-independent cross section as a function of Q^2 and at different incident beam energies. The different beam energy dependence of the DVCS^2 and BH·DVCS interference term complement the azimuthal analysis of the cross section in order to provide a complete separation of these two contribution.

Scaling of the real part of the DVCS amplitude

The Q^2-dependence of these observables will provide a strong scaling test of the *real* part of the DVCS amplitude that will complement the one obtained in E00-110 from the helicity-correlated cross section. Testing scaling on the real part of the DVCS amplitude is indeed a very stringent check. The imaginary part of the DVCS amplitude access GPDs along one kinematical line $x = \pm\xi$. In JLab kinematics $x \in [\xi, 1]$ and the twist-2 amplitude of DVCS describes the emission and absorption of a quark with different momentum fractions. The real part of the DVCS amplitude is related to GPD integrals over their full domain $-1 < x < 1$. Over the region $x \in [-\xi, \xi]$ the twist-2 amplitude correspond to the emission of a quark-antiquark pair from the initial proton, and in the region $x \in [-1, -\xi]$ one has emission and reabsorption of antiquarks. Therefore, testing the scaling properties of GPD integrals tests the twist-2 dominance of DVCS over a wide variety of partonic configurations.

Separation of the longitudinal π^0 electroproduction cross section

In addition to these fundamental measurements on DVCS, E07-007 will concurrently measure the π^0 electroproduction cross section for different beam energies. We successfully measured the π^0 electroproduction cross section in E00-110. However, since we only ran at one incident beam energy, the longitudinal and transverse separation of the cross section could not be done. E07-007 will allow the first separation of the longitudinal cross section, using the Rosenbluth technique. A factorization theorem holds for the longitudinal π^0 electroproduction cross section that relates it, at sufficiently large Q^2, to a different flavor combination of GPDs. This channel is an essential element to make a flavor decomposition of GPDs, which is impossible to obtain from DVCS on the proton alone.

E07-007 will test the Q^2-dependence of the longitudinal cross section and check if the factorization is applicable at the Q^2 values currently accessible experimentally (around $Q^2 \sim 2\,\text{GeV}^2$). If this test turns out positive, very interesting and complementary information on GPDs will be available from this channel.

E08-025: Rosenbluth-like separation on the neutron

An equivalent DVCS program at 6 GeV using a deuterium target was approved earlier this year and will run concurrently with E07-007. It will allow to separate the interference and DVCS^2 terms on neutron observables. This will complement E07-007 on the proton.

12 GEV PROGRAM

The experimental GPD program is at the heart of the scientific motivation of the major Jefferson Lab upgrade to 12 GeV.

E12-06-114 [24] is a wide experimental program of DVCS high precision cross-section measurements in Hall A with CEBAF at 12 GeV, enthusiastically approved by JLab PAC-30. With polarized 6.6, 8.8, and 11 GeV beams incident on the liquid hydrogen target, we will provide a major survey of proton DVCS in almost the entire kinematic range accessible with CEBAF at 12 GeV (Fig. 6).

REFERENCES

1. X.-D. Ji, *Phys. Rev. Lett.* **78**, 610–613 (1997), `hep-ph/9603249`.
2. A. V. Radyushkin, *Phys. Rev.* **D56**, 5524–5557 (1997), `hep-ph/9704207`.
3. D. Mueller, D. Robaschik, B. Geyer, F. M. Dittes, and J. Horejsi, *Fortschr. Phys.* **42**, 101 (1994), `hep-ph/9812448`.
4. J. C. Collins, and A. Freund, *Phys. Rev.* **D59**, 074009 (1999), `hep-ph/9801262`.
5. X.-D. Ji, and J. Osborne, *Phys. Rev.* **D58**, 094018 (1998), `hep-ph/9801260`.
6. M. Diehl, T. Gousset, B. Pire, and J. P. Ralston, *Phys. Lett.* **B411**, 193–202 (1997), `hep-ph/9706344`.
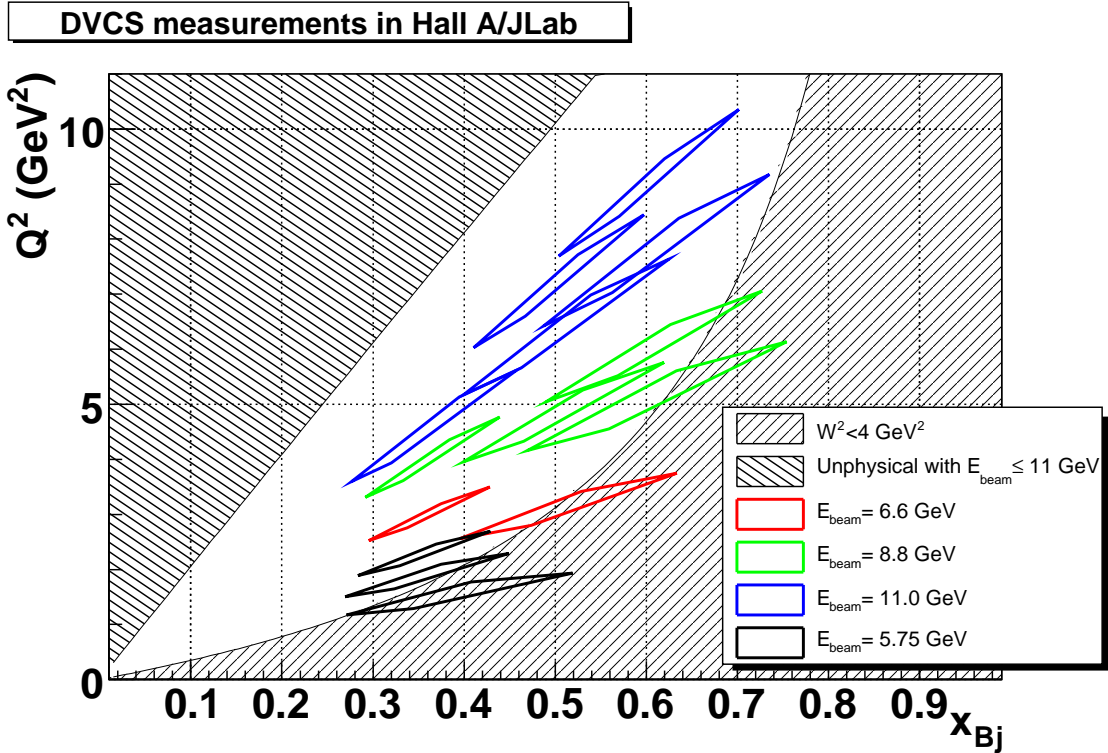7. M. Burkardt, *Phys. Rev.* **D62**, 071503 (2000), `hep-ph/0005108`.

FIGURE 6. Approved DVCS kinematics for H$(e, e'\gamma)p$ measurements in Hall A with 3, 4, and 5 pass beams of CEBAF at 12 GeV. The diamond shapes trace the approximate acceptance of the Hall A High Resolution Spectrometer in each setting. The boundary of the unphysical region corresponds to the maximum possible Q^2 at a given x_B for 11 GeV. This corresponds to 180° electron scattering, equivalent to $\theta_q = 0°$. The points at $E_{Beam} = 5.75$ GeV were obtained in E00-110.

8. J. P. Ralston, and B. Pire, *Phys. Rev.* **D66**, 111501 (2002), `hep-ph/0110075`.
9. M. Diehl, *Eur. Phys. J.* **C25**, 223–232 (2002), `hep-ph/0205208`.
10. A. V. Belitsky, X.-D. Ji, and F. Yuan, *Phys. Rev.* **D69**, 074014 (2004), `hep-ph/0307383`.
11. A. Aktas, et al., *Eur. Phys. J.* **C44**, 1–11 (2005), `hep-ex/0505061`.
12. C. Adloff, et al., *Phys. Lett. B* **517**, 47–58 (2001), `hep-ex/0107005`.
13. S. Chekanov, et al., *Phys. Lett.* **B573**, 46–62 (2003), `hep-ex/0305028`.
14. A. Airapetian, et al., *Phys. Rev. Lett.* **87**, 182001 (2001), `hep-ex/0106068`.
15. F. Ellinghaus, *Nucl. Phys.* **A711**, 171–174 (2002), `hep-ex/0207029`.
16. A. Airapetian, et al. (2006), `hep-ex/0605108`.
17. S. Stepanyan, et al., *Phys. Rev. Lett.* **87**, 182002 (2001), `hep-ex/0107043`.
18. S. Chen, et al., *Phys. Rev. Lett.* **97**, 072002 (2006), `hep-ex/0605012`.
19. C. Muñoz Camacho, et al., *Phys. Rev. Lett.* **97**, 262002 (2006), `nucl-ex/0607029`.
20. M. Mazouz, et al., *Phys. Rev. Lett.* **99**, 242501 (2007), `0709.0450`.
21. M. Vanderhaeghen, P. A. M. Guichon, and M. Guidal, *Phys. Rev.* **D60**, 094017 (1999), `hep-ph/9905372`.
22. C. Muñoz Camacho, et al. (2007), URL `http://www.jlab.org/exp_prog/proposals/07/PR-07-007.pdf`.
23. R. De Masi, et al., *Phys. Rev.* **C77**, 042201 (2008), `0711.4736`.
24. J. Roche, et al. (2006), `nucl-ex/0609015`.